Available online at www.sciencedirect.com

ScienceDirect

Procedia Engineering 156 (2016) 172 – 179

Procedia Engineering

www.elsevier.com/locate/procedia

9th International Conference „Bridges in Danube Basin 2016“, BDB 2016

GPR investigation of flexible soil-steel bridge structure

Łukasz Kosno[a]*, Łukasz Sławski[a], Grzegorz Świt[a]

[a]*Kielce University of Technology, Al. Tysiąclecia Państwa Polskiego 7, 25-314 Kielce, Poland*

Abstract

Flexible soil-steel structures are commonly used due to its advantages including quicker construction process, lower cost of erection and maintenance, architectural values and others. However its behavior differs from classic rigid structures. It may be the reason why principles of soil-steel structures' work are not always completely understood and lack of grasp may cause construction and design faults. To enable its detection and elimination non-destructive testing methods should be used. These methods are widely applied due to possibility of insight into inside of the completed structure. Nowadays, one of the most popular NDT methods is Ground Penetrating Radar method. It is commonly used in communication engineering for technical condition assessment of road and airfield pavements, railway embankments or bridge decks. To date this method is not widely used for flexible soil-steel structures' inspections. This paper shows application of GPR method for SuperCor structure study. As a result of the research series of processed radargrams were obtained. They allowed to detect construction incorrectness of backfill layers and drainage elements. Presence of these anomalies may affect the sustainability which is dependent on the proper execution of drainage system. Case study presented in this paper may be helpful in determining reasons of incorrect behavior of soil steel structures during its exploitation what was repeatedly reported by road administrators.

Peer-review under responsibility of the organizing committee of BDB 2016

Keywords: GPR; Georadar; Non-destructive testing; Soil-steel structure; Corrugated Plate; SuperCor; Bridge inspection

1. Introduction

Soil-steel structures have been in use for more than a hundred years now. They are applied as culverts, bridges, tunnels and wildlife crossings. Their work principle differs from that of classical rigid designs. Bearing capacity of flexible structures is increased due to presence of the „positive arching" phenomenon.[1,2] Differences can also be seen in the construction phase. Deformation progresses with the backfilling process; initially, the steel shell narrows and arches upwards. After construction of subsequent backfill layers above the crown, deformation decreases and steel shell returns to nearly the original shape. Due to the fact that axial forces are only present and bending moments are reduced or eliminated, the structure is regarded as pre-stressed [2,3].

* Corresponding author. *E-mail address:* lkosno@tu.kielce.pl

Peer-review under responsibility of the organizing committee of BDB 2016

doi:10.1016/j.proeng.2016.08.283

Nomenclature

c – electromagnetic wave propagation velocity in vacuum – 30.0cm/ns
ε_r – dielectric constant of a given medium
η_1 – intrinsic impedance in the first low-loss medium
η_2 – intrinsic impedance in the second low-loss medium
$\varepsilon_{r,1}$ – dielectric constant of the first medium
$\varepsilon_{r,2}$ – dielectric constant of the second medium

Due to the fact that axial forces are only present and bending moments are reduced or eliminated, the structure is regarded as pre-stressed [2,3]. Shape deformations of the structure have to be controlled rigorously. According to the guidelines issued by national roads and highways managing authority in Poland - GDDKiA[4], the allowable dimensional deviations of structure must not exceed 2% of its span. The allowable deviations of the investigated structure have noticeable rated value of 16.0cm.

It is especially important if compared with the waterproofing membrane allowable slope, which is 5%. Therefore monitoring of the structure's dimensions is a critical issue. In case of lack of proper supervision or suspicion of improper performance of the structure, its quality can be assessed using the Ground Penetrating Radar method. The GPR method can be very useful in evaluation of layers thickness, changes in density levels, location of construction members, voids, dampness and other anomalies.[5,6] The GPR data can be used for identification and detection of precarious subsurface deterioration.[7] This paper presents the case study of GPR method application to checking the construction correctness of the flexible culvert built under a provincial road in Poland in 2015.

2. Technical data of investigated structure

The investigated structure was a flexible culvert made from SuperCor SC-35B corrugated steel structure. Its basic dimension are shown below:

- length (base / crown) 30.0 / 18.60m
- width x height (inlet/outlet) 7.50 x 2.72 / 7.50 x 3.72m
- culvert axis – road axis intersection angle 90°
- road crown width 14.75m, including:
- asphalt kerbless roadway 7.0m
- right shoulder width 1.5m
- left shoulder width 1.25m
- pavement on the left side (width of 1.5m) separated from the roadway by a trapezoid-shaped ditch (width of 2.5m).

The culvert was designed for Class A (500kN) moving loading, as a flexible corrugated soil-steel structure. Foundation was made in the form of a rigid open concrete box with a variable height. The steel structure was covered with soil backfill with the parameters defined in the technical specification. The waterproofing membrane was made of two layers of geotextile separated with a layer of geomembrane. It had required slope of 5% and was ended with a drain tile. Above the layers of soil backfill, road structural layers were placed:

- wearing course, made from SMA 11 mixture (still to be placed) 4.0cm
- binding course made from asphalt concrete AC WMS22W 9.0cm
- base course, made from asphalt concrete AC 22P 12.0cm
- crack relief layer manufactured from SMA 8 mixture 4.0cm
- subbase layer made of deep recycled mineral-cement mixture (MC) class C3/4. The MC mixture was produced with the use of recycled asphalt layers derived from existing pavement, in the amount of up to 50%. The design thickness of subbase layer was 25.0cm, but during the construction process it was increased up to 50.0cm. The actual thickness of this layer is provided further in this article.

The levels of the structural elements of the culvert, given in the plans and specifications are as shown below:

- road profile (design/field value without the wearing course) 186.16/186.12
- road edge (design/field value without the wearing course) 186.09/186.05

- steel shell crown (top/bottom of the corrugation) 184.32/184.18

According to the geodetic measurement the level of the waterproofing membrane at the crown is 184.68. The total height of soil backfill and structural layers over the culvert is 180.0cm (without wearing course).

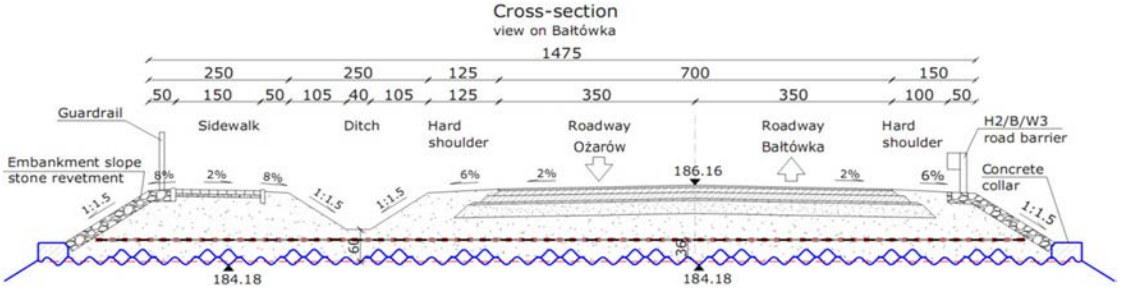

Fig. 1. Cross-section of the road layers above the investigated culvert.

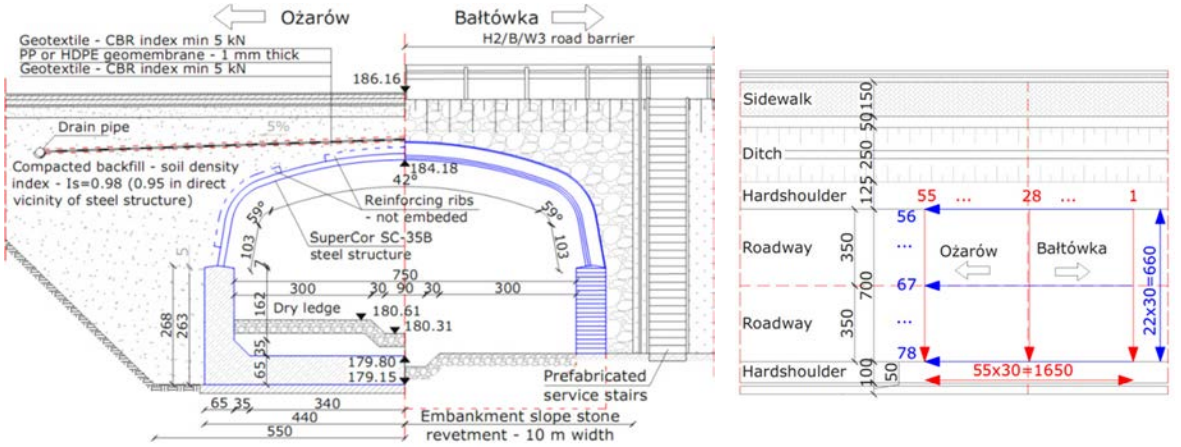

Fig. 2. (a) Longitudinal cross-section of the culvert; (b) road layout with measurement scheme.

3. Data acquisition

The Georadar survey was conducted before the final inspection of the road in November 2015 at lack of precipitation for seven days prior to the measurement. The structure was surveyed using the GPR system with 900MHz antenna. The scans were taken along and across the road axis with a spacing of 30.0cm. The value of sampling frequency was 1024 and a length of time window was 71.0ns. The scheme of the routes over the culvert is shown in Fig. 2b. As a result of the survey series of raw radargrams were obtained, which were then processed with the use of dedicated software. Filtration involved the correction of signal-to-noise ratio, correction of correlation and continuity of the reflections, elimination of determined noise and minimization of random noise. [8] However, the real shape of the steel structure was impossible to obtain due to the arch-like shape of the feature in the longitudinal cross-section and corrugation of the steel shell. This form of structure scatters waves considerably.

4. Results of the research

Estimation of structural layers thickness and its parameters requires determination of an electromagnetic wave propagation velocity in the medium. The velocities calculated with the use of dedicated software are as listed below:

- bituminous pavement layers 17.0-18.0cm/ns
- MC subbase 8.0-12.0cm/ns
- backfill layers above the waterproofing membrane 10.0cm/ns

Determination of wave propagation velocity in backfill layers below the waterproofing membrane is difficult due to lack of clear-cut signals that might be used. The discrepancies between propagation velocities are probably caused by non-uniform compaction of the material or its non-homogeneity. Calculated velocities can be compared to the quotient of the layer thickness and the propagation time. Determination of wave propagation time across consecutive layers required the use of radargrams 56 and 78, which were obtained from the edge of the roadway. These scans are not distorted by increased wave propagation velocity in the joint between the strips of MC subbase layer, in contrast to scan 67 which was obtained from the roadway profile. The wave propagation times allowed to calculate the propagation velocity. Thickness of sand backfill below the waterproofing membrane, 36cm, read from the geodetic documents was the basis for estimation of average wave propagation velocity in this layer:

$$\frac{36.0cm}{7.0ns \times 0.5} \approx 10.0cm/ns$$

The thickness of sand backfill layer above the membrane, assuming that wave propagation velocity is equal for the layers of sand backfill below and above the membrane (which are made of the same material), can be calculated:

$$10.0ns \times 0.5 \times 10.0cm/ns \approx 50.0cm$$

MC subbase layer thickness is the difference between the total surcharge thickness and the road asphalt and sand backfill layers thickness:

$$180.0cm - 25.0cm - 50.0cm - 36.0cm = 69.0cm$$

The estimated propagation velocity of electromagnetic wave for the MC layer can be calculated:

$$\frac{69.0cm}{(21.5-3.5)ns \times 0.5} \approx 8.0cm/ns$$

The estimated wave propagation velocity for the layers of the asphalt pavement (without the wearing course) is:

$$\frac{25.0cm}{(3.5-0.5)ns \times 0.5} \approx 17.0cm/ns$$

Values of the dielectric constant for the given medium can be found using the following expression:[9]

$$\varepsilon_r = \left(\frac{c}{v}\right)^2$$

Values of dielectric constant for consecutive layers are the following:
- asphalt pavement layers 3.1
- MC subbase layer 14.1
- for the sand backfill 9.0

The phenomenon of electromagnetic wave reflection allows to determine the continuity of the medium and detect the boundaries of any anomalies found. The efficiency of detection depends on reflection factor Γ, which is equal to the ratio between the amplitudes of the reflected and incident wave. The higher the contrast of intrinsic impedances, (thus of electric permittivity), the stronger the boundary separating two low-loss media reflects electromagnetic waves.[9] Reflection factor Γ should be defined by the following equation:

$$\Gamma = \frac{\eta_2 - \eta_1}{\eta_2 + \eta_1} \cong \frac{\sqrt{\varepsilon_1} - \sqrt{\varepsilon_2}}{\sqrt{\varepsilon_1} + \sqrt{\varepsilon_2}}$$

The reflection factor Γ, dependent on the relative electric permittivity, has the form:

$$\Gamma = \frac{\sqrt{\varepsilon_{r,1}} - \sqrt{\varepsilon_{r,2}}}{\sqrt{\varepsilon_{r,1}} + \sqrt{\varepsilon_{r,2}}}$$

The electromagnetic pulse propagates through the medium and reaches interface of the structural layers. If assumed value of amplitude of pulse was 1.0 then the values of amplitude of the wave reflected from the media boundary are:
- for asphalt pavement - MC subbase interface ≈ 0.36
- for the MC subbase - sand backfill interface ≈ -0.11
- for sand backfill -steel structure interface ≈ -1

In second case the wave changes polarization at the layer boundary. The remaining energy is transmitted deeper into the sand backfill. The interface can be observed only if the layers are built from materials with different dielectric constants, thus different wave propagation velocities. Here, the layers of sand backfill were prepared from the same material, thus the reflection factor Γ should be zero. Therefore the interface visible between the layers of sand backfill indicates the presence of a waterproofing membrane. The reflection factor for the sand backfill - steel structure interface is Γ= -1, due to the fact that metal is a perfect reflector. It reflects the entire wave energy and the space behind the steel shell cannot be seen.

The results of research are shown below. Processed georadar data is presented in the form of B-scans - profiles consisting single radar traces (A-scans). The scan length is marked on the horizontal axis, with wave propagation velocity on the vertical axis. In the top left hand corner, the wave amplitude and the assigned scale of grey is shown.

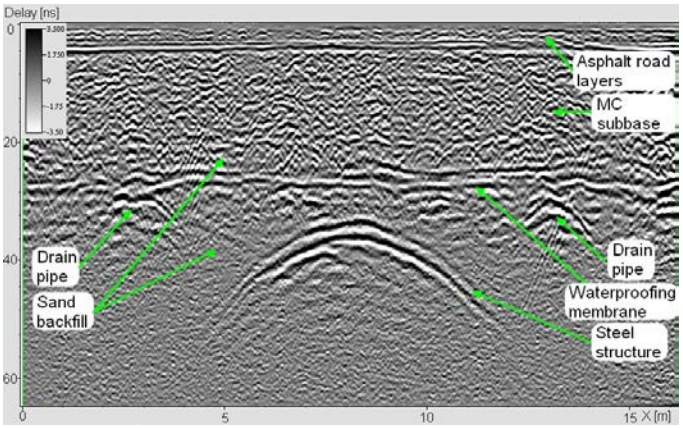

Fig. 3. Longitudinal cross-section of the culvert (scan no. 65) with structural elements indicated.

Fig. 3 presents a longitudinal cross-section of the feature attained for scan no. 65 in a vicinity of the road axis. The waterproofing membrane appears for the delay of 26.0-28.0ns, and the steel structure for the delay of 32.0ns. These elements are “elevated” relative to radargrams attained farther away from the road axis. This anomaly is the result of an increased wave propagation velocity in the medium, probably caused by lower compaction degree of a part of the MC subbase layer. The subbase was manufactured in stages and locations of the anomalies correspond to the locations of the joint between subbase strips in the road axis. The phenomenon can be observed on the scan transverse to the road axis as well as the tomography images (C-scans). Fig. 4 shows the differences in times of wave propagation between the MC subbase - sand backfill interface and waterproofing membrane interface.

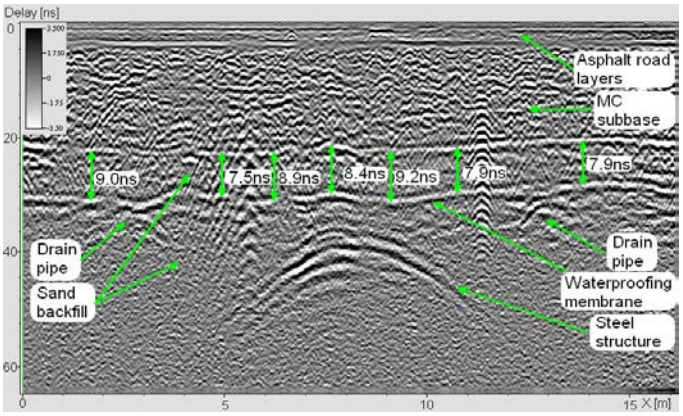

Fig. 4. Longitudinal cross-section of the culvert (scan no. 71) with differences between the electromagnetic wave propagation times of subsequent interfaces and structural elements indicated.

The interfaces that can be observed on Fig. 4 are continuous, with no traceable faults, which is especially clear in the right part of the radargram. It can be assumed that in the upper layers there are no areas of varied density or other anomalies that could have a significant influence on the wave propagation velocity. The waterproofing membrane appears for the delay of 28.0-32.0ns, and the steel structure for the delay of 35.0ns. These values match the ones on profile 74 and are noticeably higher than those on profile 65, what may indicate uniform compaction of the MC subbase layer in this area.

The electromagnetic wave propagation time, denoted between the interfaces is variable. The maximum value of 9.2ns is reached at ordinate X=9.2m. This propagation time corresponds to the thickness of 46.0cm for assumed propagation velocity of 10.0cm/ns. Another local maximum of 8.9ns is reached at ordinate X=6.0m. The distance between the layers decreases to 8.4ns above the crown of the structure, and to 7.5-7.9ns at the longer distance from it. Depressions of the waterproofing membrane appear at the sites of local maxima.

According to the detailed design the waterproofing membrane should have roof-like slope of 5%. It has to be noted that the road over the culvert has a longitudinal slope, that is the road level decreases from left to right. The slope should show the visible interfaces inclined inversely relative to the road slope. The level of the waterproofing membrane visible on the radargram should be lower on the left side of the structure and higher on the right side. However, the slope of the waterproofing membrane is opposite to the design slope on both sides of the structure.

Even at the conservative assumption that the observed interfaces are distorted by the differences in the wave propagation velocities caused by the variations in compaction degree of the layers lying higher and slope of the road, the differences in the wave propagation times in the sand backfill above the membrane, at local depressions in X=6.0 and X=9.2m, are 0.5-0.8ns relative to the crown and 1.3-1.4ns relative to the times measured for the neighbouring levels on the external side. At the assumed electromagnetic wave propagation velocity in the sand backfill of 10.0cm/ns, these values correspond to the depressions with a depth in the range 2.5-4.0cm relative to the crown and 6.5-7.0cm relative to the times measured for the levels on the external side. The design slope of the waterproofing membrane of 5.0cm/m may hinder proper drainage in the structure. This in turn may affect its service life, as stagnating water can freeze and thaw locally, causing the lifting and lowering of the layers located above and leading to degradation of the structure. Fig. 5 presents anomalies described above.

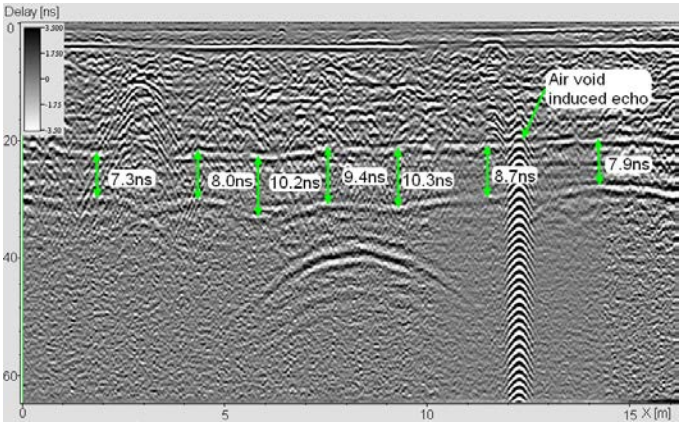

Fig. 5. Longitudinal cross-section of the culvert (scan no. 74) with differences between the wave propagation times of subsequent interfaces.

Fig. 6 presents the cross-section of the investigated culvert. The “elevation” of the steel structure, sand backfill and waterproofing membrane can be observed. This elevation is a result of the noticeable increase in the electromagnetic wave propagation velocity in the medium induced probably by the changes in compaction degree. The lines of the sand backfill-steel structure, waterproofing membrane and the MC subbase-sand backfill interface run in parallel to each other. It may suggest that the area of insufficient compaction is located in the MC subbase layer. This also implies that the sand backfill layers are homogeneous and thus uniformly compacted. This phenomenon can be observed over the entire scanning area along the road axis.

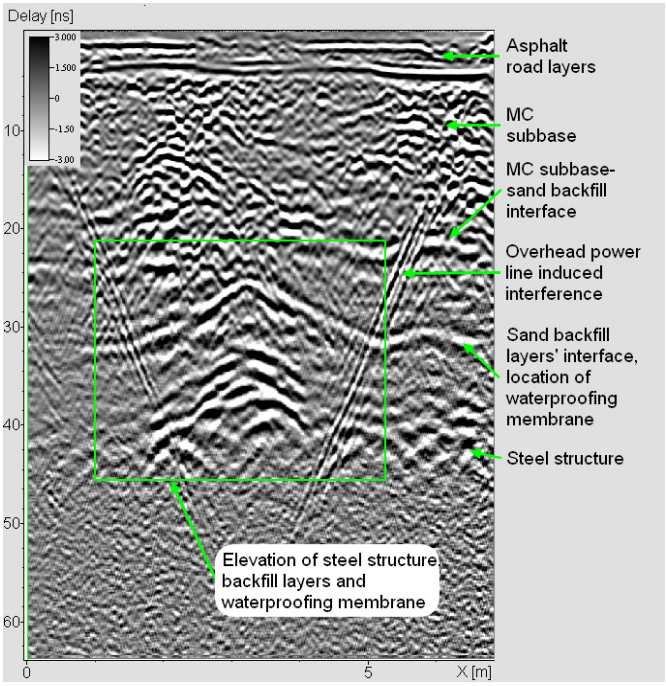

Fig. 6. Transverse cross-section of the culvert (scan no. 27) with structural elements indicated.

The tomographic images - C-scans - are generated for the delays: 9.0ns, 27.6ns, 36.6ns, and 44.0ns. The time given refers to the distance the wave propagates to the feature surveyed and back. The first image, for a delay of 9.0ns, shows a cross section of the MC subbase layer. Red colour corresponds to lower propagation velocity and higher amplitude of the wave. The semicircular shapes correspond to the regions with higher compaction degree. This pattern was probably a result of spreading piles of MC mixture supplied from the plant and compacting subsequent placement areas. It has to be noted that the scanned area covered only the roadway. This explains the asymmetry of the pattern cut off at the bottom part of the image.

Fig. 7b presents the tomographic image for delay of 27.6ns. The region of red colour running along the road axis is visible in the mid-height of the radargram. This is a portion of the waterproofing membrane interface. Elevation of its image was a result of the increase in the wave propagation velocity at the joint between the strips of MC subbase. This phenomenon also distorts the image of the lower-lying features. The centre of the steel shell, located under the subbase area with a lower degree of compaction appears on tomographic images for considerably lower delays than for the remaining portions of the steel structure, as shown on Fig. 8.

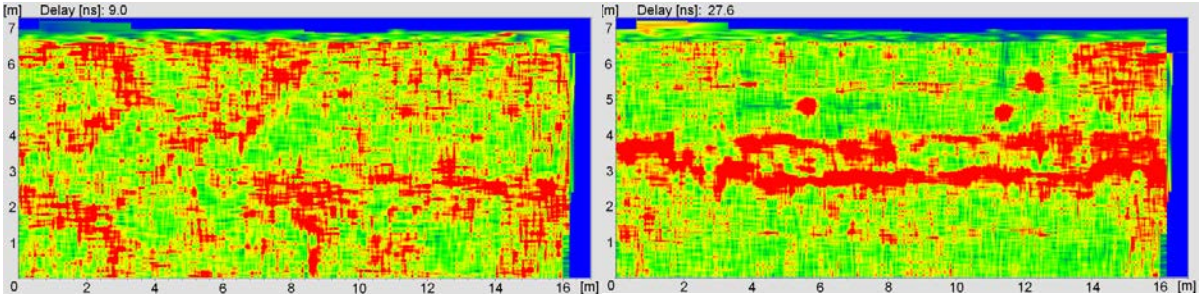

Fig. 7. (a) tomographic image generated for the delay of 9.0ns; (b) tomographic image generated for the delay of 27.6ns.

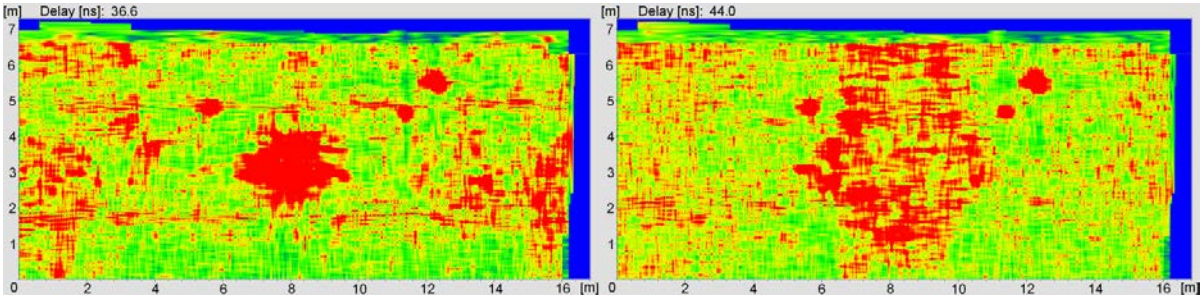

Fig. 8. (a) tomographic image generated for the delay of 36.6ns, (b) tomographic image generated for the delay of 44.0ns.

5. Conclusions

The GPR method is now one of the most popular non-destructive testing methods. It is widely used, especially in the construction of transport infrastructure, where it is applied for assessment of the condition of road and airfield pavements, railway embankments or classical bridge structures. It has to be noted that in spite of numerous advantages, this method has not been commonly used for the non-destructive testing of flexible soil-steel structures. The major limitation of georadar method, which are difficulties in interpretation of survey data, may be the reason. The application of the GPR method for the flexible soil-steel structure testing, as discussed in this article, allowed the scanning of structural layers, determining the location of drain elements and evaluating the quality of work conducted in subsurface, inaccessible depths.

The research indicated potential problems related to improper backfill drainage, which may lead to failure or even disaster due to the action of water and low temperatures. The areas with a lower degree of compaction were also detected.

The GPR method may be of considerable value in the case of flexible soil-steel structures. It can be used as an efficient tool for the evaluation of the quality of work done (final inspection) and for the identification of poor workmanship when there is a need for further, more detailed tests with the use of, for example, a lightweight dynamic penetrometer. The GPR surveys can also be a helpful tool for the evaluation of technical condition of existing structures and while planning the range of repair works to be done.

References:

[1] Janusz L., Madaj A., Obiekty inżynierskie z blach falistych. Projektowanie i wykonawstwo, Wydawnictwa Komunikacji i Łączności, Warszawa, 2007.
[2] Machelski Cz., Modelowanie mostowych konstrukcji gruntowo-powłokowych, Dolnośląskie Wydawnictwo Edukacyjne, Wrocław 2008.
[3] Kosno Ł., Świt G. Behaviour analysis of steel-shell-and-soil corrugated structure in the construction phase illustrated with SuperCor SC-57S, Conference Proceedings, p. 716-722, 24TH International Conference on Metallurgy and Materials Metal2015, Brno, Czech Republic
[4] Generalna Dyrekcja Dróg Krajowych i Autostrad, Zalecenia projektowe i technologiczne dla podatnych konstrukcji inżynierskich z blach falistych, Załącznik do Zarządzenia Nr 9 Generalnego Dyrektora Dróg Krajowych i Autostrad z dn. 18 marca 2004r, Żmigród 2004.
[5] Annan, A.P., GPR For infrastructure imaging, , Symposium Proceedings BB 85-CD, 6TH International Symposium on Non-Destructive Testing in Civil Engineering NDT-CE 2003, Berlin, Germany
[6] Hugenschmidt J., Non-destructive-testing of traffic-infrastructure using GPR, Symposium Proceedings BB 85-CD, 6THInternational Symposium on Non-Destructive Testing in Civil Engineering NDT-CE 2003, Berlin, Germany
[7] Goszczyńska B., Świt G., Trąmpczyński W., Monitoring of Active Destructive Processes as a Diagnostic Tool for the Structure Technical State Evaluation, Bulletin of the Polish Academy of Sciences, 2013, Volume: 61, Issue: 1, p.: 97-109.
[8] Kosno Ł. at al., Inwentaryzacja niedostępnych elementów konstrukcji budynku z zastosowaniem georadaru na przykładzie budynku zabytkowego, monografia z 61. Konferencji Naukowej Bydgoszcz-Krynica, 20-25.09.2015, p.: 85-91.
[9] Karczewski J., Zarys metody georadarowej. Uczelniane wydawnictwo naukowo – dydaktyczne AGH, Kraków, 2007.